

How many-body correlations and α -clustering shape ${}^6\text{He}$

Carolina Romero-Redondo,^{1,*} Sofia Quaglioni,^{1,†} Petr Navrátil,^{2,‡} and Guillaume Hupin³

¹*Lawrence Livermore National Laboratory, P.O. Box 808, L-414, Livermore, California 94551, USA*

²*TRIUMF, 4004 Wesbrook Mall, Vancouver, British Columbia, V6T 2A3, Canada*

³*CEA, DAM, DIF, F-91297 Arpajon, France.*

(Dated: April 5, 2024)

The Borromean ${}^6\text{He}$ nucleus is an exotic system characterized by two halo neutrons orbiting around a compact ${}^4\text{He}$ (or α) core, in which the binary subsystems are unbound. The simultaneous reproduction of its small binding energy and extended matter and point-proton radii has been a challenge for *ab initio* theoretical calculations based on traditional bound-state methods. Using soft nucleon-nucleon interactions based on chiral effective field theory potentials, we show that supplementing the model space with ${}^4\text{He}+n+n$ cluster degrees of freedom largely solves this issue. We analyze the role played by the α -clustering and many-body correlations, and study the dependence of the energy spectrum on the resolution scale of the interaction.

PACS numbers: 21.60.De, 25.10.+s, 27.20.+n

Introduction. Achieving a comprehensive and unified treatment of many-body correlations and clustering in atomic nuclei constitutes a frontier for contemporary nuclear theory. A light exotic nucleus that has been challenging our understanding of such complex phenomena based on nucleonic degrees of freedom and high-quality models of their interactions (i.e., within an *ab initio* framework) is Helium-6 (${}^6\text{He}$). This is a prominent example of Borromean quantum ‘halo’, i.e. a weakly-bound state of three particles ($\alpha+n+n$) otherwise unbound in pairs, characterized by “large probability of configurations within classically forbidden regions of space” [1]. In the last few years, its binding energy [2] and charge radius [3] have been experimentally determined with high precision. The ${}^6\text{He}$ ground state (g.s.) is also of great interest for tests of fundamental interactions and symmetries. Precision measurements of its β -decay half life have recently taken place [4] and efforts are under way to determine the angular correlation between the emitted electron and neutrino [5]. To date, traditional *ab initio* bound-state calculations can successfully describe the interior of the ${}^6\text{He}$ wave function [6–10], but are unable to fully account for its three-cluster asymptotic behavior. At the same time, the only *ab initio* study of $\alpha+n+n$ dynamics naturally explains the asymptotic configurations, but underbinds the ${}^6\text{He}$ g.s. owing to missing many-body correlations [11, 12]. As a result, a comprehensive description of the ${}^6\text{He}$ g.s. properties is still missing.

In this Letter we present a study of the ${}^6\text{He}$ g.s. in which both six-body correlations and clustering are successfully addressed by means of the no-core shell model with continuum (NCSMC) [13]. This approach, introduced to describe binary processes starting from two- [14, 15] and later three-body [16–18] Hamiltonians, is here generalized to the treatment of three-cluster dynamics. We further explore the role of six-body correlations in the description of the low-lying $\alpha+n+n$ continuum, required to accurately evaluate the ${}^4\text{He}(2n,\gamma){}^6\text{He}$ radiative

capture (one of the mechanism by which stars can overcome the instability of the five- and eight-nucleon systems and create heavier nuclei [19]) and of the ${}^3\text{H}({}^3\text{H}, 2n){}^4\text{He}$ reaction contributing to the neutron yield in inertial confinement fusion experiments [20, 21].

Approach. In the NCSMC, the A -nucleon wave function of a system characterized by a *core*+ $n+n$ asymptotic in the total angular momentum, parity and isospin channel $J^\pi T$ is written as the generalized cluster expansion

$$|\Psi^{J^\pi T}\rangle = \sum_{\lambda} c_{\lambda}^{J^\pi T} |A\lambda J^\pi T\rangle + \sum_{\nu} \iint dx dy x^2 y^2 G_{\nu}^{J^\pi T}(x, y) \hat{A}_{\nu} |\Phi_{\nu xy}^{J^\pi T}\rangle, \quad (1)$$

where $c_{\lambda}^{J^\pi T}$ and $G_{\nu}^{J^\pi T}(x, y)$ are, respectively, discrete and continuous variational amplitudes to be determined, $|A\lambda J^\pi T\rangle$ is the square-integrable (antisymmetric) solution for the λ -th energy eigenstate of the system obtained working within the A -body harmonic oscillator (HO) basis of the no-core shell model (NCSM) [22],

$$|\Phi_{\nu xy}^{J^\pi T}\rangle = \left[(|A-2 \lambda_c J_c^{\pi_c} T_c\rangle (|n\rangle |n\rangle)^{(s_{nn} T_{nn})})^{(ST)} \right. \\ \left. \times (Y_{\ell_x}(\hat{\eta}_{nn}) Y_{\ell_y}(\hat{\eta}_{c,nn}))^{(L)} \right]^{(J^\pi T)} \frac{\delta(x - \eta_{nn})}{x \eta_{nn}} \frac{\delta(y - \eta_{c,nn})}{y \eta_{c,nn}} \quad (2)$$

are continuous microscopic-cluster states [11] describing the organization of the nucleons into an $(A-2)$ -nucleon *core* and two neutrons $|n\rangle$, and \hat{A}_{ν} is an appropriate inter-cluster antisymmetrizer introduced to preserve the Pauli exclusion principle. The *core* eigenstates are also computed in the NCSM, employing the same HO frequency $\hbar\Omega$ and consistent number of quanta above the lowest energy configuration N_{\max} used for the A -nucleon system. The states of Eq. (2) are labeled by the quantum numbers $\nu = \{A-2 \lambda_c J_c^{\pi_c} T_c; s_{nn} T_{nn} S \ell_x \ell_y L\}$. Furthermore, $\vec{\eta}_{c,nn} = \eta_{c,nn} \hat{\eta}_{c,nn}$ and $\vec{\eta}_{nn} = \eta_{nn} \hat{\eta}_{nn}$ are Jacobi relative coordinates proportional to the separation between the center of mass (c.m.) of the *core* and that of

the residual two neutrons, and to the neutrons' relative position, respectively.

Similar to the binary-cluster case [15], upon orthogonalization of expansion (1), we obtain the unknown $c_\chi^{J^\pi T}$ and $G_\nu^{J^\pi T}(x, y)$ amplitudes by solving the Schrödinger equation in the model space spanned by the basis states $|A\lambda J^\pi T\rangle$ and $\mathcal{A}_\nu |\Phi_{\nu xy}^{J^\pi T}\rangle$. However, given the additional relative coordinate, in the three-cluster case we first express the continuous amplitudes in the orthogonalized expansion (i.e., the relative-motion wave functions) in terms of the hyperradius $\rho = \sqrt{x^2 + y^2}$ and hyperangle $\alpha = \arctan \frac{x}{y}$ and expand them in the hyperangular basis $\phi_K^{\ell_x \ell_y}(\alpha)$ analogously to Ref. [11]. The ${}^6\text{He}$ g.s. energy and wave function $|\Psi_{\text{g.s.}}\rangle$, as well as the matrix elements of the $\alpha+n+n$ scattering matrix are found by matching the orthogonalized form of expansion (1) with the known asymptotic behavior of the wave function using an extension of the microscopic R -matrix method on Lagrange mesh [15, 23–27]. We obtain convergence of the hyperangular expansion and R -matrix method using the same parameters as in Refs. [11, 12]. We then analyze the hyperradial components of the $\alpha+n+n$ relative motion and preferred spatial configurations within the g.s. of ${}^6\text{He}$. To this end, we perform a projection of $|\Psi_{\text{g.s.}}\rangle$ into the orthogonalized cluster basis (2), i.e.,

$$\begin{aligned} \sum_{\nu'} \iint dx' dy' x'^2 y'^2 \mathcal{N}_{\nu\nu'}^{-1/2}(x, y, x', y') \langle \Psi_{\text{g.s.}} | \mathcal{A}_\nu | \Phi_{\nu' x' y'}^{J^\pi T} \rangle \\ = \frac{1}{\rho^{5/2}} \sum_K \tilde{u}_{\nu K}(\rho) \phi_K^{\ell_x \ell_y}(\alpha), \end{aligned} \quad (3)$$

where $\mathcal{N}_{\nu\nu'}(x, y, x', y')$ is the overlap between the antisymmetrized states (2) [11]. Finally, we obtain the matter (r_m) and point-proton (r_{pp}) root-mean-square (rms) radii by computing the square root of the expectation values on the g.s. wave function of the operators

$$r_m^2 \equiv \frac{1}{A} \sum_{i=1}^A r_i^2 = \frac{1}{A} \rho^2 + \frac{A-2}{A} r_m^{2(c)}, \quad (4)$$

and

$$r_{pp}^2 \equiv \frac{1}{Z} \sum_{i=1}^A r_i^2 \frac{(1 + \tau_i^{(3)})}{2} = r_{pp}^{2(c)} + R^{2(c)}, \quad (5)$$

respectively. Here Z is the total number of protons, $\tau_i^{(3)}$ is the third component of isospin and r_i the distance from the A -nucleon c.m. of the i th nucleon, $r_m^{2(c)}$ and $r_{pp}^{2(c)}$ are *core* operators defined analogously to Eqs. (4) and (5), respectively, and $R^{(c)} = \sqrt{\frac{2}{A(A-2)}} \eta_{c,nn}$ is the distance between the c.m. of the *core* and that of the whole system. The expressions on the far right-hand side of Eqs. (4) and (5) are used to compute the matrix elements involving the microscopic-cluster portion of the basis and were

specifically derived for *core*+ $n+n$ partitions. In particular, the formulation of Eq. (5) is only valid for the present case of isospin $T_c = 0$ *core*. A more detailed account of the formalism will follow in a separate publication [28].

Results. We start from the chiral N^3LO nucleon-nucleon (NN) interaction of Ref. [29] softened via the similarity renormalization group (SRG) method [30–32], which minimizes momentum components above a given resolution scale Λ . In particular we work with $\Lambda = 2.0 \text{ fm}^{-1}$. In nuclei up to mass number $A = 6$ this momentum resolution leads to binding energies close to experiment despite the omission of the three-nucleon ($3N$) components of the SRG-transformed chiral Hamiltonian [33], and has been shown to induce negligible (less than 1%) two- and higher-body corrections of the ${}^3\text{H}$ and ${}^4\text{He}$ matter radii computed with bare operators [34]. In the interest of showcasing the vast improvement of the present approach over the use of expansions based exclusively on $\alpha+n+n$ microscopic-cluster states, we also perform calculations with the even softer $\Lambda = 1.5 \text{ fm}^{-1}$ resolution scale adopted in our earlier studies of Refs. [11, 12]. Calculations for $\Lambda = 1.5$ and 2.0 fm^{-1} were carried out using the same $\hbar\Omega = 14$ and 20 MeV HO frequencies of Refs. [11, 12] and [17], respectively. All results were obtained including only the $J_c^\pi T_c = 0^+0$ g.s. of the α particle and the first four, three and two square-integrable eigenstates of the six-nucleon system for the $J^\pi = 0^+, 1^\pm$ and 2^+ channels, respectively.

As shown in Table I, convergence for the ${}^6\text{He}$ g.s. energy computed within the NCSMC is achieved within less than 10 keV for $\Lambda = 1.5 \text{ fm}^{-1}$, and the result is in excellent agreement with the infinite-space extrapolation of the NCSM [11]. This and the good agreement with the accurate extrapolated value of Ref. [8] give us reason to believe that convergence is achieved in the largest model space considered also for the harder ($\Lambda = 2.0 \text{ fm}^{-1}$) interaction. In general, the ${}^4\text{He}(\text{g.s.})+n+n$ degrees of freedom efficiently account for the onset of clustering already

TABLE I. Computed ${}^6\text{He}$ g.s. energies in MeV for the $\Lambda = 1.5$ and 2.0 fm^{-1} interactions as a function of the absolute HO model space size $N_{\text{tot}} = N_0 + N_{\text{max}}$, where N_0 is the number of quanta shared by the nucleons in their lowest configuration. For the ${}^4\text{He}(\text{g.s.})+n+n$ calculation of Ref. [11], $N_0 = 0$. However, for the the p -shell ${}^6\text{He}$ nucleus within the NCSM and NCSMC, $N_0 = 2$. The last two rows show NCSM extrapolated results, and the experimental value, respectively.

		$\Lambda = 1.5 \text{ fm}^{-1}$		$\Lambda = 2.0 \text{ fm}^{-1}$	
N_{tot}	Ref. [11]	NCSM	NCSMC	NCSM	NCSMC
6	-28.91	-27.71	-30.02	-26.44	-28.64
8	-28.62	-28.95	-29.69	-27.70	-28.81
10	-28.70	-29.45	-29.86	-28.37	-28.97
12	-28.70	-29.66	-29.86	-28.72	-29.17
∞	—	-29.84(4) [11]	—	-29.20(11) [8]	—
Exp.		-29.268			

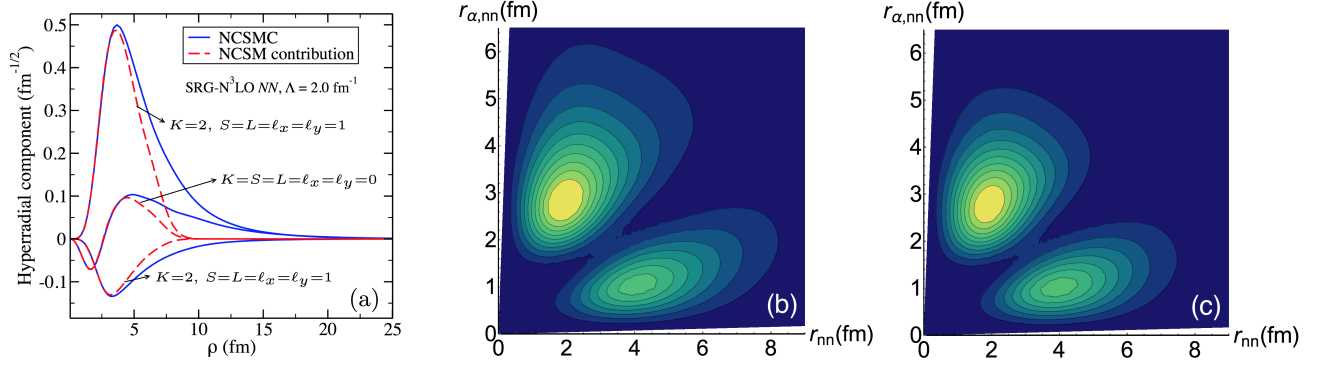


FIG. 1. (Color online) Panel (a): Most relevant hyperradial components $\tilde{u}_{\nu K}(\rho)$ of the $\alpha+n+n$ relative motion [see Eq.(3)] within the ${}^6\text{He}$ g.s. after projection of the $\Lambda = 2.0 \text{ fm}^{-1}$ full NCSMC wave function in the largest model space (blue solid lines) as well as of its NCSM portion (red dashed lines) into the orthogonalized microscopic-cluster basis. Panel (b) and (c): Contour plots of the probability distribution obtained from the projection of the full NCSMC wave function of panel (a) and its NCSM component, respectively, as a function of the relative coordinates $r_{nn} = \sqrt{2}\eta_{nn}$ and $r_{\alpha,nn} = \sqrt{3/4}\eta_{\alpha,nn}$.

in small model spaces. Conversely, the square-integrable eigenstates supply many-body correlations that are not accounted for in a microscopic-cluster expansion including only the g.s. of ${}^4\text{He}$, such as the one shown in the first column of the table (note that ${}^6\text{He}$ is unbound in the analogous calculations for $\Lambda = 2.0 \text{ fm}^{-1}$). As shown in Fig. 1(a), the ${}^4\text{He}(\text{g.s.})+n+n$ portion of the basis serves also the important role of providing the correct asymptotic behavior and extended configurations of the hyper-radial motion typical of a Borromean halo such as ${}^6\text{He}$.

The projection over the orthogonalized microscopic-cluster basis of Eq. (3) captures 97% of the original NCSMC solution, confirming the $\alpha+n+n$ picture of the ${}^6\text{He}$ g.s. To visualize its spatial structure, we present in Fig. 1(b) the contour plot of the associated probability distribution. This displays the characteristic dominance of the “di-neutron” configuration (two neutrons about 2 fm apart orbiting the *core* at a distance of about 3 fm) over the “cigar” picture (two neutrons far from each other with the α particle in between) already seen in numerous previous studies [8, 11, 23, 35–38]. While these structures are already captured by the square-integrable portion of the basis [see Fig. 1(c)], they are more spatially extended in the full calculation.

The rms matter and point-proton radii obtained from the computed NCSMC g.s. wave functions using the more ‘realistic’ $\Lambda = 2.0 \text{ fm}^{-1}$ momentum resolution are shown

together with the corresponding two-neutron separation energy (S_{2n}) in Fig. 2 and summarized in Table II. Also shown as shaded bands are the accurate S_{2n} measurement of Ref. [2], the range of experimental matter radii spanned by the values and associated error bars of Refs. [39–41], and the bounds for the point-proton radius as evaluated in Ref. [7] from the charge radius reported in Ref. [3]. All three observables exhibit a considerably weaker dependence on the size of the HO basis compared

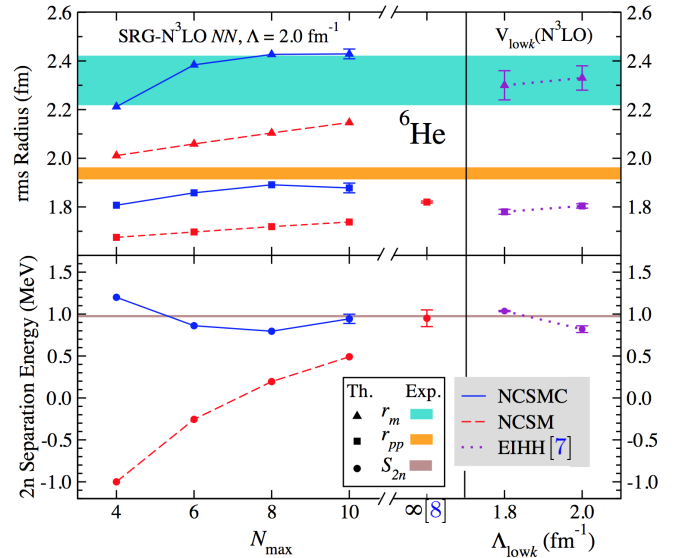


FIG. 2. (Color online) NCSMC (blue solid lines) and NCSM (red dashed lines) rms matter (triangles) and point-proton (squares) radii, and two-neutron separation energy (circles), obtained using the SRG- $N^3\text{LO}$ NN interaction with $\Lambda = 2.0 \text{ fm}^{-1}$ as a function of the HO basis size. Also shown are the infinite-basis extrapolations from Ref. [8] and the EIH results from Ref. [7] at the resolution scales $\Lambda_{\text{lowk}} = 1.8$, and 2.0 fm^{-1} . The range of experimental values are represented by horizontal bands (see text for more details).

TABLE II. Summary of the results presented in Fig. 2, with Λ_{lowk} in units of fm^{-1} . See text for further details.

		S_{2n} (MeV)	r_m (fm)	r_{pp} (fm)
NCSMC	($N_{\text{max}} = 10$)	0.94(5)	2.43(2)	1.88(2)
NCSM [8]	($N_{\text{max}} = \infty$)	0.95(10)	—	1.820(4)
EIHH [7]	($\Lambda_{\text{lowk}} = 2.0$)	0.82(4)	2.33(5)	1.804(9)
Exp.		0.975	2.32(10)	1.938(23)

microscopic-cluster picture, can be interpreted as a consequence of excitations of the α core. This work sets the stage for the *ab initio* study of the ${}^6\text{He}$ β -decay half-life and ${}^4\text{He}(2n, \gamma){}^6\text{He}$ radiative capture, and is a stepping stone in the calculation of the ${}^3\text{H}({}^3\text{H}, 2n){}^4\text{He}$ fusion.

Computing support for this work came from the LLNL institutional Computing Grand Challenge program. Prepared in part by LLNL under Contract DE-AC52-07NA27344. This material is based upon work supported by the U.S. Department of Energy, Office of Science, Office of Nuclear Physics, under Work Proposal No. SCW1158, and by the NSERC Grants No. 401945-2011 and SAPIN-2016-00033. TRIUMF receives federal funding via a contribution agreement with the National Research Council of Canada.

* romeroredond1@llnl.gov

† quaglioni1@llnl.gov

‡ navratil@triumf.ca

- [1] A. S. Jensen, K. Riisager, D. V. Fedorov, and E. Garrido, *Rev. Mod. Phys.* **76**, 215 (2004).
- [2] M. Brodeur, T. Brunner, C. Champagne, S. Ettenauer, M. J. Smith, A. Lapierre, R. Ringle, V. L. Ryjkov, S. Bacca, P. Delheij, G. W. F. Drake, D. Lunney, A. Schwenk, and J. Dilling, *Phys. Rev. Lett.* **108**, 052504 (2012).
- [3] L.-B. Wang, P. Mueller, K. Bailey, G. W. F. Drake, J. P. Greene, D. Henderson, R. J. Holt, R. V. F. Janssens, C. L. Jiang, Z.-T. Lu, T. P. O'Connor, R. C. Pardo, K. E. Rehm, J. P. Schiffer, and X. D. Tang, *Phys. Rev. Lett.* **93**, 142501 (2004).
- [4] A. Knecht, R. Hong, D. W. Zumwalt, B. G. Delbridge, A. García, P. Müller, H. E. Swanson, I. S. Towner, S. Utsumo, W. Williams, and C. Wrede, *Phys. Rev. Lett.* **108**, 122502 (2012).
- [5] A. Garcia and O. Naviliat-Cuncic, (2016), private communication.
- [6] S. D. Pieper, *Riv. Nuovo Cimento* **31**, 709 (2008).
- [7] S. Bacca, N. Barnea, and A. Schwenk, *Phys. Rev.* **C86**, 034321 (2012).
- [8] D. Sääf and C. Forssén, *Phys. Rev. C* **89**, 011303 (2014).
- [9] M. A. Caprio, P. Maris, and J. P. Vary, *Phys. Rev. C* **90**, 034305 (2014).
- [10] C. Constantinou, C. A. Caprio, J. P. Vary, and P. Maris, arXiv.1605.04976.
- [11] S. Quaglioni, C. Romero-Redondo, and P. Navrátil, *Phys. Rev.* **C88**, 034320 (2013) and Erratum (submitted).
- [12] C. Romero-Redondo, S. Quaglioni, P. Navrátil, and G. Hupin, *Phys. Rev. Lett.* **113**, 032503 (2014).
- [13] P. Navrátil, S. Quaglioni, G. Hupin, C. Romero-Redondo, and A. Calci, *Physica Scripta* **91**, 053002 (2016).
- [14] S. Baroni, P. Navrátil, and S. Quaglioni, *Phys. Rev. Lett.* **110**, 022505 (2013).
- [15] S. Baroni, P. Navrátil, and S. Quaglioni, *Phys. Rev. C* **87**, 034326 (2013).
- [16] G. Hupin, S. Quaglioni, and P. Navrátil, *Phys. Rev. C* **90**, 061601 (2014).
- [17] G. Hupin, S. Quaglioni, and P. Navrátil, *Phys. Rev. Lett.* **114**, 212502 (2015).
- [18] J. Langhammer, P. Navrátil, S. Quaglioni, G. Hupin, A. Calci, and R. Roth, *Phys. Rev. C* **91**, 021301 (2015).
- [19] F. Käppeler, F.-K. Thielemann, and M. Wiescher, *Annual Review of Nuclear and Particle Science* **48**, 175 (1998), <http://dx.doi.org/10.1146/annurev.nucl.48.1.175>.
- [20] D. T. Casey *et al.*, *Phys. Rev. Lett.* **109**, 025003 (2012).
- [21] D. B. Sayre *et al.*, *Phys. Rev. Lett.* **111**, 052501 (2013).
- [22] P. Navrátil, J. P. Vary, and B. R. Barrett, *Phys. Rev. C* **62**, 054311 (2000).
- [23] P. Descouvemont, C. Daniel, and D. Baye, *Phys. Rev. C* **67**, 044309 (2003).
- [24] P. Descouvemont, E. Tursunov, and D. Baye, *Nucl. Phys.* **A765**, 370 (2006).
- [25] D. Baye, J. Goldbeter, and J.-M. Sparenberg, *Phys. Rev. A* **65**, 052710 (2002).
- [26] M. Hesse, J. Roland, and D. Baye, *Nucl. Phys.* **A709**, 184 (2002).
- [27] M. Hesse, J.-M. Sparenberg, F. V. Raemdonck, and D. Baye, *Nucl. Phys.* **A640**, 37 (1998).
- [28] C. Romero-Redondo, S. Quaglioni, P. Navrátil, and G. Hupin, “Three-cluster dynamics within the *ab initio* no-core shell model with continuum,” (2016), (In preparation).
- [29] D. R. Entem and R. Machleidt, *Phys. Rev. C* **68**, 041001 (2003).
- [30] S. K. Bogner, R. J. Furnstahl, and R. J. Perry, *Phys. Rev. C* **75**, 061001 (2007).
- [31] R. Roth, S. Reinhardt, and H. Hergert, *Phys. Rev. C* **77**, 064003 (2008).
- [32] F. Wegner, *Ann. Phys.* **506**, 77 (1994).
- [33] E. D. Jurgenson, P. Navrátil, and R. J. Furnstahl, *Phys. Rev. C* **83**, 034301 (2011).
- [34] M. D. Schuster, S. Quaglioni, C. W. Johnson, E. D. Jurgenson, and P. Navrátil, *Phys. Rev. C* **90**, 011301 (2014).
- [35] I. Bida and F. Nunes, *Nucl. Phys.* **A847**, 1 (2010).
- [36] V. Kukulin, V. Krasnopolsky, V. Voronchev, and P. Sazonov, *Nucl. Phys.* **A453**, 365 (1986).
- [37] M. Zhukov, B. Danilin, D. Fedorov, J. Bang, I. Thompson, and J. Vaagen, *Phys. Rep.* **231**, 151 (1993).
- [38] E. Nielsen, D. Fedorov, A. Jensen, and E. Garrido, *Physics Reports* **347**, 373 (2001).
- [39] I. Tanihata, D. Hirata, T. Kobayashi, S. Shimoura, K. Sugimoto, and H. Toki, *Phys. Lett.* **B289**, 261 (1992).
- [40] G. D. Alkhazov *et al.*, *Phys. Rev. Lett.* **78**, 2313 (1997).
- [41] O. Kiselev *et al.*, *The European Physical Journal A - Hadrons and Nuclei* **25**, 215 (2005).
- [42] X. Mougeot, V. Lapoux, W. Mittig, N. Alamanos, F. Auger, *et al.*, *Phys. Lett.* **B718**, 441 (2012).
- [43] Centroids E_R and widths Γ are obtained, respectively, as the values of $E_{\text{kin}} = E - E_{th(\alpha+n+n)}$ for which the first derivative $\delta'(E_{\text{kin}})$ of the eigenphase shifts is maximal and $\Gamma=2/\delta'(E_R)$.
- [44] I. J. Thompson and F. M. Nunes, *Nuclear Reactions for Astrophysics* (Cambridge University Press, 2009) p. 301.
- [45] Extrapolated values E_∞ are obtained from fitting the $N_{\text{max}} = 6$ to 12 energies at $\hbar\Omega = 14$ MeV with the function $E(N_{\text{max}})=E_\infty+a \exp(-b N_{\text{max}})$.